Front. Med. 2022, 16(2): 240–250
https://doi.org/10.1007/s11684-021-0909-7

RESEARCH ARTICLE

Accurate quantification of 3′-terminal 2′-O-methylated small RNAs by utilizing oxidative deep sequencing and stem-loop RT-qPCR

Yan Kong[1], Huanhuan Hu[1], Yangyang Shan[1], Zhen Zhou[1], Ke Zen[1], Yulu Sun[3], Rong Yang (✉)[2], Zheng Fu (✉)[1], Xi Chen (✉)[1,4]

[1]Nanjing Drum Tower Hospital Center of Molecular Diagnostic and Therapy, State Key Laboratory of Pharmaceutical Biotechnology, Jiangsu Engineering Research Center for MicroRNA Biology and Biotechnology, NJU Advanced Institute of Life Sciences (NAILS), Institute of Artificial Intelligence Biomedicine, School of Life Sciences, Nanjing University, Nanjing 210023, China; [2]Department of Urology, Drum Tower Hospital, Medical School of Nanjing University, Institute of Urology, Nanjing University, Nanjing 210008, China; [3]Department of General Surgery, Drum Tower Hospital, Medical school of Nanjing University, Nanjing 210008, China; [4]Research Unit of Extracellular RNA, Chinese Academy of Medical Sciences, Nanjing 210023, China

Abstract **The continuing discoveries of novel classes of RNA modifications in various organisms have raised the need for improving sensitive, convenient, and reliable methods for quantifying RNA modifications. In particular, a subset of small RNAs, including microRNAs (miRNAs) and Piwi-interacting RNAs (piRNAs), are modified at their 3′-terminal nucleotides via 2′-O-methylation. However, quantifying the levels of these small RNAs is difficult because 2′-O-methylation at the RNA 3′-terminus inhibits the activity of polyadenylate polymerase and T4 RNA ligase. These two enzymes are indispensable for RNA labeling or ligation in conventional miRNA quantification assays. In this study, we profiled 3′-terminal 2′-O-methyl plant miRNAs in the livers of rice-fed mice by oxidative deep sequencing and detected increasing amounts of plant miRNAs with prolonged oxidation treatment. We further compared the efficiency of stem-loop and poly(A)-tailed RT-qPCR in quantifying plant miRNAs in animal tissues and identified stem-loop RT-qPCR as the only suitable approach. Likewise, stem-loop RT-qPCR was superior to poly(A)-tailed RT-qPCR in quantifying 3′-terminal 2′-O-methyl piRNAs in human seminal plasma. In summary, this study established a standard procedure for quantifying the levels of 3′-terminal 2′-O-methyl miRNAs in plants and piRNAs. Accurate measurement of the 3′-terminal 2′-O-methylation of small RNAs has profound implications for understanding their pathophysiologic roles in biological systems.**

Keywords small RNAs; 2′-O-methylation; sequencing; RT-qPCR

Introduction

The deposition of chemical modifications at specific sites of ribonucleic acid (RNA) molecules is a ubiquitous phenomenon in all kingdoms of life [1]. More than 170 distinct RNA modifications have currently been identified in different organisms [2,3], and the methylation of the ribose moiety at the 2′-hydroxyl group (2′-O-methylation) is one of the most common and abundant RNA modifications. 2′-O-methylation is present in almost all types of cellular RNAs, including tRNAs (tRNAs), rRNAs (rRNAs), mRNAs (mRNAs), small nuclear/small nucleolar RNAs (snRNAs/snoRNAs), and different small RNAs. 2′-O-methylation increases the structural diversity of cellular RNAs and has the potential to alter their function and stability [4,5].

In particular, a subset of eukaryotic small RNAs is modified at their 3′-terminal nucleotides via 2′-O-methylation. In plants, the biogenesis of microRNAs (miRNAs), which refer to a class of endogenous single-stranded small noncoding RNAs of 19–25 nucleotides in length that play critical roles in regulating gene expression at post-transcriptional levels [6,7], involves 2′-O-methylation at their 3′-termini by a S-adenosylmethionine-dependent methyltransferase called Hua enhancer 1 (HEN1) [8].

Received May 12, 2021; accepted November 25, 2021
Correspondence: Xi Chen, xichen@nju.edu.cn;
Zheng Fu, zhengfu@nju.edu.cn;
Rong Yang, doctoryr@gmail.com

Moreover, Piwi-interacting RNAs (piRNAs), which refer to a class of germ cell-specific small RNAs of 26–31 nucleotides in length that form clusters at hundreds of genome locations and function in protecting the animal germline by silencing transposons [9–11], are 2′-O-methylated at their 3′-termini by HEN1 homologs [12–15]. In *Drosophila*, endogenous small interfering RNAs (endo-siRNAs), which refer to a class of ~22 nucleotide-long small RNAs that are usually derived from endogenous, long RNA duplexes after being cleaved by Dicer [16,17], are modified by the methyltransferase DmHen1 at their 3′-termini [12]. 2′-O-methylation at the 3′-terminus is vital for the biological functions of these small RNAs to protect small RNAs from 3′ nucleotide addition [8,13,18–20], which probably stimulates a 3′-5′ exonucleolytic activity to degrade the tagged small RNAs. Additionally, the artificial introduction of 3′-terminal 2′-O-methylation in siRNAs increases the stability of siRNAs *in vivo* without affecting their RNA interference activities [12,19].

The ubiquitous presence of 3′-terminal 2′-O-methyl modifications across a wide variety of small RNAs raises the need for methods that can detect and quantitate the expression levels of modified small RNAs reliably. Unfortunately, quantifying the 3′-terminal 2′-O-methylated small RNAs directly is difficult [21], mainly owing to the 2′-O-methylation at the 3′-termini of RNAs negatively affecting the enzymatic activity of polyadenylate polymerase and T4 RNA ligase, which are the two enzymes that are required for RNA labeling or ligation in commercial miRNA profiling assays [22]. That is, if a sample is a mixture of 2′-O-methyl and 2′-OH small RNAs, then RNA labeling and ligation would favor the capture of the 2′-OH small RNAs, thereby introducing a considerable detection bias toward lower levels of 3′-terminal 2′-O-methylated small RNAs [23]. Thus, accurate measurement of 3′-terminal 2′-O-methyl-modified small RNAs remains a paramount challenge. For instance, although accumulating lines of evidence have demonstrated that plant miRNAs can influence gene expression and cellular processes in mammals as dietary miRNAs derived from food [24–31], some studies have failed to detect exogenous miRNAs from consumed plants in animal blood and tissues [32–35]. Since mammalian miRNAs have far less 2′-O-methylation than plants [8,36], mammalian miRNAs are much easier to be detected than methylated plant miRNAs in these tissues. Unsurprisingly, plant miRNAs were missed in these studies when inappropriate methods were used for the plant miRNA detection in animal tissues. Likewise, deep sequencing technology detected very minimal accumulation of 2′-O-methyl piRNAs in seminal plasma compared with more enriched 2′-OH miRNAs; however, stem-loop RT-qPCR technology generated contradictory results [23]. Indeed, monitoring the dynamic change in the 3′-terminal 2′-O-methylation of small RNAs during various biological processes is difficult because of the lack of an accurate quantification method. Considering that determining the absolute levels of 3′-terminal 2′-O-methyl modifications in small RNA metabolism is of great importance to further understand their biological functions, the development of a reliable and accurate approach is urgently needed to minimize the bias related to RNA 3′-terminal 2′-O-methylation and to analyze the level of 3′-terminal 2′-O-methylated small RNAs quantitatively.

In the present study, we compared the efficiency of various widely used RNA quantification tools in measuring 3′-terminal 2′-O-methylated small RNAs. We developed a feasible strategy by which the 3′-terminal 2′-O-methyl levels of small RNAs can be quantified accurately. With this strategy, we determined the levels of plant miRNAs in rice-fed mice and piRNAs in human seminal plasma successfully.

Materials and methods

Animals

All experimental animals were maintained on a C57BL/6J background on a 12-h light/dark cycle in a pathogen-free animal facility at Nanjing University. The Institutional Review Board of Nanjing University approved all housing and surgical procedures. At 6 weeks of age, each mouse was fed fresh rice by gavage after fasting overnight. The mice were maintained on this diet for 3 days, after which serum and tissues were collected. Several mice were euthanized directly after overnight fasting, and their sera and tissues were collected as a control.

Semen samples

All samples were collected according to protocols approved by the Medical Ethics Committee of Nanjing Drum Tower Hospital. Semen samples were collected from healthy donors. Informed consent was obtained from each patient before sperm collection. Semen samples were collected into a 15 mL centrifuge tube after 3–5 days of sexual abstinence and liquefied for 30 min at 37 °C. Seminal plasma was obtained by centrifuging semen samples at room temperature at 3000 rpm for 10 min, and the supernatant was then collected and stored at −80 °C until analysis.

Synthetic miRNA oligonucleotides

Synthetic miRNA and piRNA oligonucleotides, including 2′-OH miRNAs and piRNAs and 3′-terminal 2′-O-methyl miRNAs and piRNAs, were purchased from GenePharma (Shanghai, China). Oligonucleotide powder was dissolved in diethylpyrocarbonate (DEPC) water to generate a 20 μmol/L stock solution and stored at −80 °C. Synthetic unmethylated or methylated plant miRNA standards (e.g.,

miR156a, miR158a, miR159a, miR166a, and miR168a) were mixed with synthetic unmethylated animal miRNA standards (e.g., miR-16, miR-21, and miR-122). The concentration of each plant miRNA was 10^{-2} μmol/L, and the concentration of each animal miRNA was 10^{-1} μmol/L. Synthetic unmethylated or methylated piRNA standards (e.g., piR-30198, piR-31068, piR-31925, piR-43771, and piR-42773) were mixed with synthetic unmethylated animal miRNA standards (e.g., miR-16, miR-21, miR-122, miR-423, and let-7a) according to the above protocol. The concentration of each piRNA was 10^{-1} μmol/L, and the concentration of each animal miRNA was 10^{-1} μmol/L. The sequences of all oligonucleotides used are listed in Table S1.

RNA extraction

Total RNA was extracted from serum, seminal plasma, and tissues using TRIzol Reagent (Invitrogen) according to the manufacturer's instructions. A total of 50–100 mg tissue was ground with 1 mL TRIzol Reagent in a tissue grinding apparatus. Liver tissues were obtained from 6-week-old male C57BL/6J mice. For seminal plasma, 100 μL of sample was mixed with 1 mL of TRIzol Reagent in a 1.5 mL microcentrifuge tube (RNase-free). The mixture was vortex-mixed vigorously and then added to 0.02 pmol synthetic MIR2911(GenePharma). The mixture was further vortex-mixed vigorously, and 200 μL of chloroform was then added. The mixture was vortexed, incubated on ice for 10 min, and then centrifuged at 16 000× *g* for 20 min at 4 °C. The supernatant was transferred to a new 1.5 mL microcentrifuge tube. Then, the same volume of isopropanol was added to the supernatant, and the tube was inverted 10 times to mix thoroughly. Subsequently, the mixture was stored at −20 °C for 1 h followed by centrifugation at 16 000× *g* and 4 °C for 20 min. After discarding the supernatant, the pellet was washed with 1 mL 75% ethanol and centrifuged again at 16 000× *g* and 4 °C for 20 min. The pellet was then dried for 20 min at room temperature. Finally, the pellet was dissolved in 20–50 μL DEPC water and stored at −80 °C until further analysis.

Oxidation of small RNAs with sodium periodate

Periodate oxidation was performed, as previously described but with slight modifications [8,37]. Briefly, total RNA was extracted from mouse liver using TRIzol Reagent (Invitrogen) according to the manufacturer's instructions. A 100 μL mixture that consisted of 30 μg of total RNA and 80 mmol/L NaIO4 was incubated at 4 °C for 40 or 90 min in the dark. The oxidized RNA was purified by a kit (ZYMO) and then subjected to RNA deep sequencing.

RNA deep sequencing

The methylation status of small RNAs was evaluated by treating small RNAs with sodium periodate followed by RNA deep sequencing. Briefly, after the PAGE purification of small RNA molecules under 30 bases and ligation of a pair of adaptors to their 5′ and 3′ ends, the small RNA molecules were amplified using adaptor primers for 17 cycles, and fragments of approximately 90 bp (small RNA + adaptors) were isolated from agarose gels. The purified DNA was used directly for cluster generation and sequencing analysis using Illumina's Sequencer according to the manufacturer's instructions. Then, the image files generated by the sequencer were processed to produce digital-quality data. The subsequent procedures involved the summarization of the generated data, the evaluation of sequencing quality, and the calculation of the length distribution of small RNA reads. Finally, clean reads were compared with the miRBase database (release 22), and the total copy number of each sample was normalized to 1 000 000.

RT-qPCR assays

Two RT-qPCR systems were used in our research: stem-loop primer system and poly(A)-tailed system. A TaqMan probe-based RT-qPCR assay for miRNA detection was performed according to the manufacturer's instructions (LightCycler480; Applied Biosystems), with a minor modification, as described previously [38,39]. Briefly, the reverse transcription reaction was carried out in 10 μL containing 0.5−1 μg of RNA extract, 1 μL of 10 mmol/L dNTPs, 0.5 μL of AMV reverse transcriptase (TaKaRa), 1 μL of a stem-loop RT primer (Applied Biosystems), 2 μL of 5× reverse transcription buffer, and diethylpyrocarbonate (DEPC) water. For cDNA synthesis, the reaction mixtures were incubated at 16 °C for 30 min, 42 °C for 30 min, and 85 °C for 5 min and then held at 4 °C. Real-time PCR was performed (1 cycle of 95 °C for 5 min and 40 cycles of 95 °C for 15 s and 60 °C for 1 min) with an Applied Biosystems LightCycler480 Detection System. The reaction was performed with a final volume of 20 μL containing 1 μL of cDNA, 0.3 μL of Taq, 0.33 μL of hydrolysis probe (Applied Biosystems), 1.2 μL of 25 mmol/L $MgCl_2$, 0.4 μL of 10 mmol/L dNTPs, 2 μL of 10× PCR buffer, and 14.77 μL of DEPC water.

The poly(A)-tailed RT-qPCR assay for miRNA detection was performed according to the manufacturer's instructions (Qiagen). The reverse transcription system included 10× miScript Nucleics Mix, 5× miScript HiSpec Buffer, and miScript Reverse Transcriptase Mix. Samples were kept on ice before running the programs. The reverse transcription program was detailed as follows: 37 °C for 60 min and 95 °C for 5 min and then held at 4 °C. After obtaining cDNAs, 2× QuantiTect SYBR Green Master Mix, 10× miScript Universal Primer, and 10× miScript Primer Assay were used for real-time PCR detection. The primer sequences of the poly(A)-tailed RT-qPCR method are

shown in Table S2. The program was presented as follows: 95 °C for 15 min, followed by 40 cycles of 94 °C for 15 s, 55 °C for 30 s, and 70 °C for 30 s. Each cDNA sample was tested in triplicate.

For piRNA detection, the system and procedure of the tailed PCR method were the same as those of miRNA detection. For the stem-loop system, the reverse transcription reaction was carried out in 10 μL containing 0.5−1 μg of extracted RNA, 0.5 μL of 10 mmol/L dNTPs, 0.5 μL of AMV reverse transcriptase (TaKaRa), 1 μL of a stem-loop RT primer (GenePharma), 2 μL of 5× reverse transcription buffer, and 0.25 μL of recombinant RNase inhibitor (RRI) and diethylpyrocarbonate (DEPC) water. For the synthesis of cDNA, the reaction mixtures were incubated at 16 °C for 15 min, 42 °C for 60 min, and 85 °C for 5 min and then held at 4 °C. Real-time PCR was performed (1 cycle of 95 °C for 5 min and 40 cycles of 95 °C for 15 s and 60 °C for 1 min) with an Applied Biosystems LightCycler480 Detection System. The reaction was performed with a final volume of 20 μL containing 1 μL of cDNA, 0.3 μL of Taq, 0.4 μL of 10 μmol/L primer (GenePharma), 0.2 μL of probe (GenePharma), 1.2 μL of 25 mmol/L $MgCl_2$, 0.4 μL of 10 mmol/L dNTPs, 2 μL of 10× PCR buffer, and 14.5 μL of DEPC water.

Statistical analysis

The analyses were performed using GraphPad Prism 8. The data are presented as the mean ± SEM of at least three independent experiments, and differences were considered statistically significant at $P < 0.05$ using two-tailed Student's *t*-tests.

Results

Profiling 3′-terminal 2′-O-methylated miRNAs from consumed plants in animal tissues by oxidative deep sequencing

Deep sequencing is superior to other conventional tools in capturing the whole genome-wide expression profiles of small RNA species. Unfortunately, the 2′-O-methyl modification at the 3′-terminus of small RNAs results in decreased efficiency of adaptor ligation, so the sequencing procedure is biased against 3′-terminal 2′-O-methylated small RNAs compared with 3′-terminal 2′-OH small RNAs [22]. Therefore, the sequencing reads of 2′-O-methyl small RNAs will be lost in the basal pool of unmodified small RNAs [23]. However, after treatment with sodium periodate (oxidizing agent), the cis-diol ribose groups of unmodified miRNAs will be destroyed and converted into dialdehydes, whereas 3′-terminal 2′-O-methylation enables miRNAs to resist periodate. Consequently, only 3′-terminal 2′-O-methylated RNAs contribute to the sequencing library, whereas the oxidized ribose groups of unmodified miRNAs are not competent for 3′-adapter ligation and are therefore excluded from the generated library [8]. Theoretically, 3′-terminal 2′-O-methyl small RNAs should be detected preferentially, and the basal pool of unmodified small RNAs should be decreased in oxidative deep sequencing, to allow the enrichment of 3′-terminal 2′-O-methylated small RNAs in the obtained sequencing reads. Given that we have previously reported that plant miRNAs can be ingested from plant food sources, pass through the gastrointestinal tract, enter the blood, accumulate in tissues, and regulate endogenous gene expression in mammals [24], we fed mice with rice and treated the total RNA isolated from mouse liver with sodium periodate for 40 or 90 min. Subsequently, the RNA samples were repurified and subjected to deep sequencing. As anticipated, most animal miRNAs in mouse liver had an unmodified 3′-terminal 2′-OH and were therefore oxidized and failed to be sequenced (Fig. 1A). In contrast, plant miRNAs in mouse liver were resistant to the oxidizing agent and were successfully detected by deep sequencing (Fig. 1B). Interestingly, when we gradually increased the oxidizing procedure from 40 to 90 min, we observed that while 40 min of treatment with oxidizing agent only partially increased plant miRNAs in mouse liver, 90 min of oxidation generated a more thorough accumulation of plant miRNAs in mouse liver (Fig. 1B). For example, animal miRNAs, such as miR-122-5p, miR-423-5p, miR-10a, miR-486-5p, miR-16-5p, miR-21-5p, miR-27b-3p, miR-30e-3p, miR-222-3p, and miR-378i, underwent a marked reduction in mouse liver after treatment with oxidizing agent, whereas plant miRNAs, such as miR156a-5p, miR159a, miR157a-5p, miR162a-3p, miR166a-3p, miR164b-5p, miR167a-5p, miR168a-5p, miR396a, and miR858a, exhibited gradually enhanced levels along with extended oxidizing time (Fig. 1C and 1D). These results indicate that the relative abundance of plant miRNAs is indeed detected by oxidative deep sequencing.

Determining the absolute levels of 3′-terminal 2′-O-methylated miRNAs from consumed plants in animal blood and tissues by RT-qPCR

Stem-loop and poly(A)-tailed RT-qPCR are common methods for quantifying small RNAs. In theory, poly(A)-tailed RT-qPCR rather than stem-loop RT-qPCR will show the reduced amplification of 3′-terminal 2′-O-methylated miRNAs [40], because the presence of a 2′-O-methyl group at the 3′-terminus may reduce the efficiency of RNA polyadenylation by polyA polymerase, whereas stem-loop primers allow the direct measurement of small RNAs independent of a 3′-terminal 2′-O-methyl modification (Fig. 2A). We synthesized several plant miRNAs (e.g., miR156a, miR158a, miR159a, miR166a, and miR168a) artificially and modified them with a 2′-O-methyl end or retained their 2′-OH ends. Then, these synthetic plant miRNAs were serially diluted and assessed using the stem-loop or poly(A)-tailed RT-qPCR assay to generate a standard curve. Stem-loop and poly(A)-tailed RT-qPCR

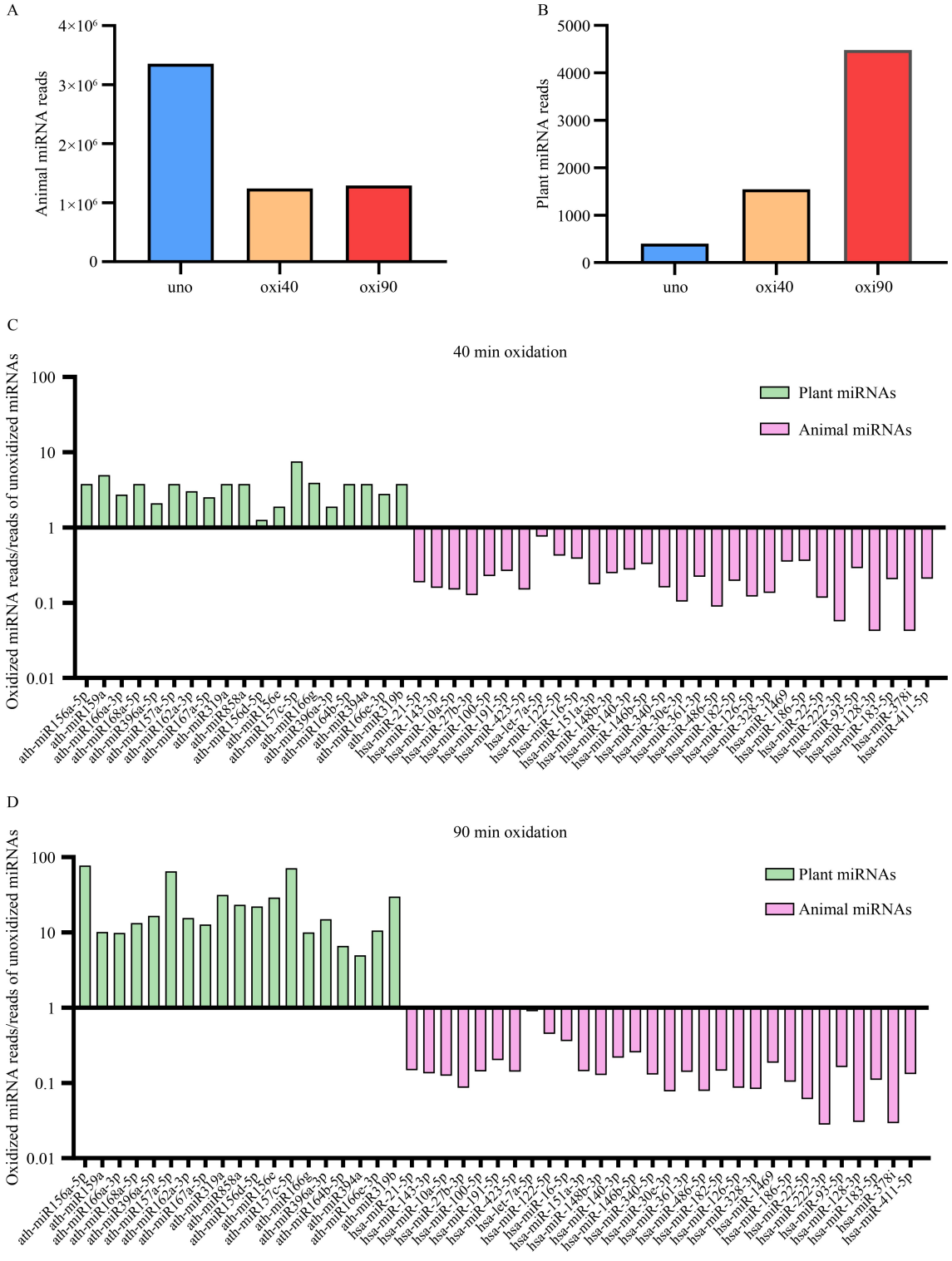

Fig. 1 Plant miRNAs in the liver of rice-fed mice are detected by oxidative deep sequencing. (A) The levels (total sequencing reads) of animal miRNAs in the livers of rice-fed mice that were unoxidized or oxidized for 40 or 90 min. For normalization, the total sequencing reads of animal miRNAs were normalized to the clean reads of each sample. (B) The levels (total sequencing reads) of plant miRNAs in the livers of rice-fed mice that were unoxidized or oxidized for 40 or 90 min. For normalization, the total sequencing reads of plant miRNAs were normalized to the clean reads of each sample. (C) Relative fold changes of plant and animal miRNAs that were subjected to 40 min of oxidation in comparison with those without oxidation. The sequencing reads of each miRNA were normalized to the clean reads of each sample. (D) Relative fold changes of plant and animal miRNAs that were subjected to 90 min of oxidation in comparison with those without oxidation. The sequencing reads of each miRNA were normalized to the clean reads of each sample.

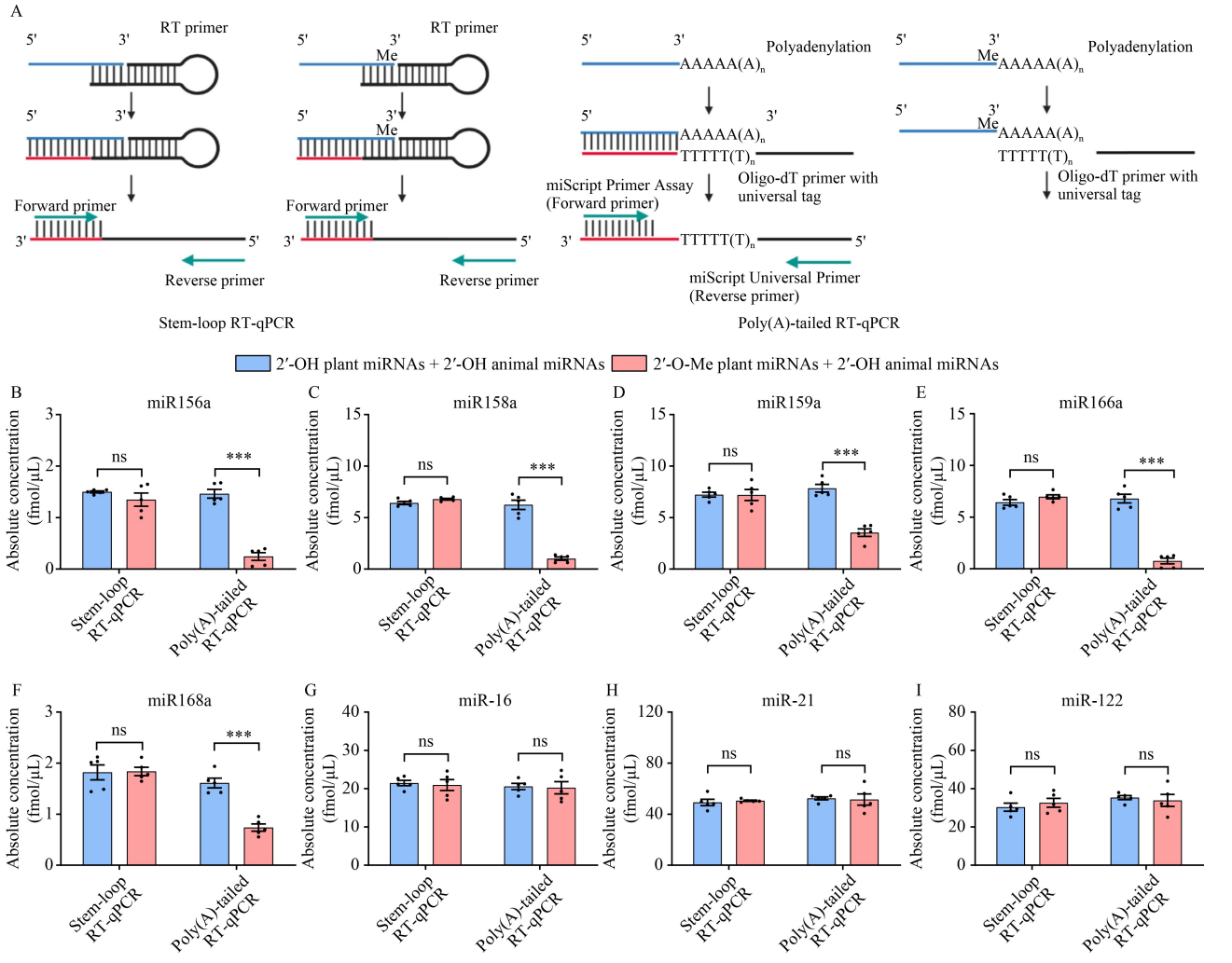

Fig. 2 Comparison of the differences between stem-loop and poly(A)-tailed RT-qPCR in quantifying synthetic 2′-O-methyl plant miRNAs. (A) Schematic diagram of the working model of stem-loop and poly(A)-tailed RT-qPCR. The blue line represents the template miRNA. The black structure or line represents the reverse transcription primer. The red line represents the reverse transcription product. The green line represents the forward primers or reverse primers. "Me" represents the methylation site. (B–F) The absolute levels of 5 synthetic 2′-O-methyl and 2′-OH plant miRNAs (miR156a, miR158a, miR159a, miR166a, and miR168a) detected by stem-loop and poly(A)-tailed RT-qPCR. (G–I) The absolute levels of 3 synthetic 2′-OH animal miRNAs (miR-16, miR-21, and miR-122) detected by stem-loop and poly(A)-tailed RT-qPCR. Data are represented as the mean ± SEM. ***$P < 0.001$.

assays showed a linear correlation between the Ct value and miRNA concentration (Fig. S1). The standard curves for stem-loop RT-qPCR analysis of unmethylated and methylated plant miRNAs nearly overlapped with each other (Fig. S1A–S1E), indicating that the stem-loop RT-qPCR assay had the same efficiency in amplifying 2′-O-methyl and 2′-OH plant miRNAs. In contrast, the poly(A)-tailed RT-qPCR assay resulted in a significant decrease in the amplification of 2′-O-methyl plant miRNAs compared with 2′-OH plant miRNAs (Fig. S1F–S1J).

Next, we compared the differences between stem-loop and poly(A)-tailed RT-qPCR in quantifying equal amounts of 2′-O-methyl and 2′-OH plant miRNAs. Synthetic unmethylated or methylated plant miRNAs were mixed with synthetic unmethylated animal miRNAs, and the mixture was quantified with stem-loop or poly(A)-tailed RT-qPCR assays. The absolute concentration of each miRNA was then calculated according to the standard curve. The stem-loop RT-qPCR assay detected equal amounts of unmethylated and methylated plant miRNAs in the mixture, whereas poly(A)-tailed RT-qPCR detected significantly lower amounts of methylated plant miRNA than unmethylated plant miRNAs (Fig. 2B–2F). As a control, stem-loop and poly(A)-tailed RT-qPCR assays detected the same amounts of nonmethylated animal miRNAs (Fig. 2G–2I). Thus, poly(A)-tailed RT-qPCR had a significantly decreased ability to quantify 2′-O-methyl miRNAs because of the presence of 3′-terminal 2′-O-methylation, whereas stem-loop RT-qPCR may be a nonbiased technique for detecting 2′-O-methyl and 2′-OH

miRNAs with equal detection efficiency.

Subsequently, we extracted RNA from the serum and liver of rice-fed mice and compared the efficiency of stem-loop and poly(A)-tailed RT-qPCR assays in differentiating 2′-O-methyl plant miRNAs from 2′-OH animal miRNAs. We first calculated the ΔCt value (recorded as Ct_{tail}−$Ct_{stem\text{-}loop}$) of each miRNA (Fig. S2). For 2′-O-methylated plant miRNAs, ΔCt values were generally larger than "zero," whereas the ΔCt values of animal miRNAs tended to be "zero." The results indicate that poly(A)-tailed RT-qPCR generated higher Ct values than stem-loop RT-qPCR when quantifying 2′-O-methyl plant miRNAs. Then, the absolute concentration of each miRNA was calculated according to the standard curve. The absolute levels of miR156a and miR168a determined by stem-loop RT-qPCR assay were significantly higher in the serum and liver of rice-fed mice than control mice (Fig. 3A, 3B, 3F, and 3G). In contrast, the poly(A)-tailed RT-qPCR assay was inefficient in detecting 2′-O-methyl plant miRNAs in rice-fed and control mice, and no significant difference in 2′-O-methyl plant miRNA levels was observed between the two groups (Fig. 3A, 3B, 3F, and 3G). As a control, the absolute levels of animal miRNAs (e.g., miR-16, miR-21, and miR-122) measured by stem-loop and poly(A)-tailed RT-qPCR showed no significant difference between the rice-fed mice and control mice (Fig. 3C, 3E, 3H, and 3J). Overall, the results confirm that the poly(A)-tailed RT-qPCR assay significantly underestimated the levels of 2′-O-methyl miRNAs.

Determining the absolute levels of 3′-terminal 2′-O-methylated piRNAs in seminal plasma by RT-qPCR

Considering that the 3′-terminal 2′-O-methylation of piRNAs also reduces the efficiency of RNA polyadenylation by polyA polymerase, poly(A)-tailed RT-qPCR analysis is biased against piRNAs compared with other nonmodified small RNAs [23]. We synthesized several piRNA sequences (e.g., piR-30198, piR-31068, piR-31925, piR-43771, and piR-42773) with 2′-O-methyl or 2′-OH ends, and the standard curves of unmethylated and methylated piRNAs were generated using stem-loop or poly(A)-tailed RT-qPCR assays (Fig. S3). Although the standard curves generated by stem-loop RT-qPCR analysis of unmethylated and methylated piRNAs largely overlapped (Fig. S3A−S3E), the standard curves generated by poly(A)-tailed RT-qPCR analysis of methylated piRNAs were significantly shifted to the right compared with those of unmethylated piRNAs (Fig. S3F−3J). We also compared the differences between stem-loop and poly(A)-tailed RT-qPCR in quantifying equal amounts of 2′-O-methyl and 2′-OH piRNAs. Unmethylated and methylated piRNAs were synthesized and mixed with unmethylated animal miRNAs. While the stem-loop RT-qPCR assay detected nearly identical levels of unmethylated and methylated piRNA in the mixture, the poly(A)-tailed RT-qPCR assay detected significantly lower levels of methylated piRNA than unmethylated piRNAs (Fig. 4A−4E). Similarly, no significant difference was observed between the two methods in detecting unmethylated animal miRNAs (Fig. 4F−4J).

Finally, we compared the efficiency of stem-loop RT-qPCR and poly(A)-tailed RT-qPCR assays in measuring 3′-terminal 2′-O-methyl piRNAs and 3′-terminal 2′-OH miRNAs in seminal plasma. The ΔCt values of piR-31068, piR-31925, piR-43771, and piR-42773 were larger than "zero," whereas the ΔCt values of miR-16, miR-21, miR-122, miR-423, and let-7a were close to "zero" (Fig. S4). Accordingly, the seminal plasma concentrations of piRNAs determined by stem-loop RT-qPCR assay were dramatically higher than those determined by poly(A)-tailed RT-qPCR assay (Fig. 4K), whereas the seminal plasma concentrations of miR-16, miR-21, miR-122, miR-423, and let-7a determined by these two approaches were quite similar (Fig. 4L). The results suggest that the 2′-O-methylation modification in piRNAs also affected detection by the poly(A)-tailed RT-qPCR approach, but the stem-loop RT-qPCR approach could overcome the interference.

Discussion

Small RNAs, 20−30 nucleotides long, have diverse and important biological roles in eukaryotic organisms [7,8,41,42]. Three major types of small RNAs, namely, miRNAs, piRNAs, and endo-siRNAs, are further modified at their 3′-terminal nucleotides via 2′-O-methylation [4,5]. To analyze these 3′-terminal 2′-O-methyl small RNAs quantitatively, several approaches have been pursued. For example, oxidative deep sequencing has already been established and widely used in piRNA research [43–45]. Unfortunately, these methods are usually limited to qualitative analysis rather than quantitative analysis or have the disadvantage of detecting low levels of small RNAs. Moreover, the most convincing analytical method to validate the presence of 3′-terminal 2′-O-methylation in small RNAs is sodium periodate oxidation combined with Northern blot [8], but this technology is labor intensive and time consuming and has relatively low throughput and sensitivity. Likewise, although mass spectrometry is a definitive tool to identify small RNA 2′-O-methylation [37], this technology yields little quantitative information and requires a substantial amount of input RNA. Also, although deep sequencing is a high-throughput and highly sensitive method to analyze small RNAs qualitatively, the presence of 2′-O-methyl modification at the 3′-terminus is known to reduce the efficiency of 3′-adapter ligation,

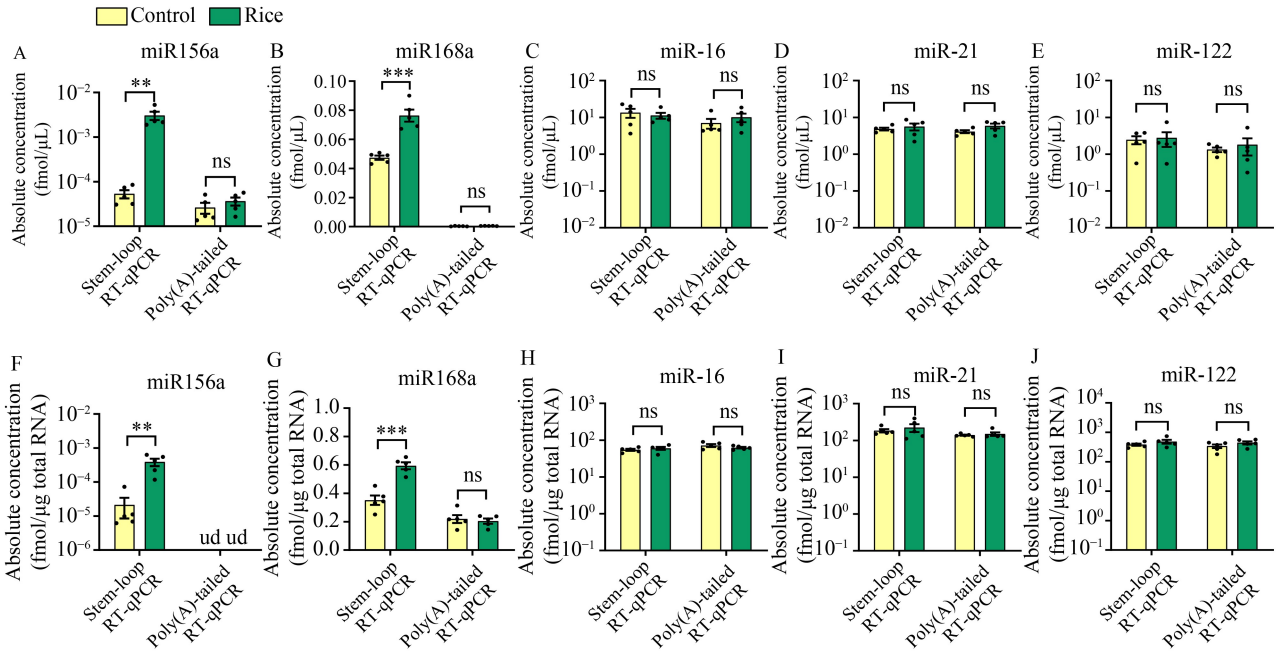

Fig. 3 Comparison of the differences between stem-loop and poly(A)-tailed RT-qPCR in quantifying 2′-O-methyl plant miRNAs in rice-fed animals. (A and B) The absolute levels of plant miRNAs (e.g., miR156a and miR168a) determined by stem-loop and poly(A)-tailed RT-qPCR in the serum of rice-fed mice. (C–E) The absolute levels of animal miRNAs (e.g., miR-16, miR-21, and miR-122) determined by stem-loop and poly(A)-tailed RT-qPCR in the serum of rice-fed mice. (F and G) The absolute levels of plant miRNAs (miR156a and miR168a) determined by stem-loop and poly(A)-tailed RT-qPCR in the livers of rice-fed mice. miRNA levels were normalized to the total amount of RNA. (H–J) The absolute levels of animal miRNAs (e.g., miR-16, miR-21, and miR-122) determined by stem-loop and poly(A)-tailed RT-qPCR in the livers of rice-fed mice. miRNA levels were normalized to the total amount of RNA. Data are represented as the mean ± SEM (n = 5). $^{**}P < 0.01$, $^{***}P < 0.001$.

thereby further reducing the library yield and representativity [22,23]. Therefore, a strategy should be optimized to improve the sensitivity of small RNA sequencing and to overcome the technical obstacles in sequencing small RNAs with 3′-terminal 2′-O-methylation. The methodology of detecting 3′-terminal 2′-O-methylated RNA has also been proposed by other groups. Brett Robb *et al.* provided a strategy to make a library by using PEG, RNL2tr, and other optimized reaction conditions. The strategy was validated by quantifying representative miRNAs and piRNAs in RNA samples prepared from mouse testes [22]. However, the customized library construction process may have limited practice of this method because most sequencing companies will not consider these customized requirements. In this study, by using the oxidative deep sequencing we not only successfully detected the level of 2′-O-methyl piRNA with higher concentration in seminal plasma, but also detected the levels of 2′-O-methyl plant miRNAs in animal tissues, where the methylated plant miRNAs existed in a lower abundance. Besides, the treatment of samples can be easily performed in any laboratory. However, given the complex procedure of periodate oxidation and RNA repurification before library construction during oxidative deep sequencing, a large amount of starting RNA material might be required. Considering that 3′-terminal 2′-O-methylated small RNAs are usually expressed at a low abundance in tissue and cellular samples, we instead applied a stem-loop RT-qPCR strategy because this approach has been reported as a highly sensitive method in amplifying the limited amount of 3′-terminal 2′-O-methylated small RNAs [46,47]. Indeed, we showed that the 2′-O-methyl plant miRNAs and piRNAs can be directly quantified on the basis of stem-loop RT-qPCR technique. Unlike poly(A)-tailed RT-qPCR, stem-loop RT-qPCR can overcome the bias related to RNA 3′-terminal 2′-O-methylation and is especially suitable for quantifying 3′-terminal 2′-O-methylated small RNAs. In addition, our results indicated that the poly(A)-tailed method is far less sensitive than stem-loop method in detecting low amount of plant miRNA in animal tissues (Fig. 3B and 3F). Thus, oxidative deep sequencing combined with stem-loop RT-qPCR may be an optimal solution to quantify 3′-terminal 2′-O-methyl small RNAs comprehensively.

Many studies have shown that dietary exogenous miRNAs can be detected in and play active roles in animal tissues [24–31]. Conversely, some studies failed to detect dietary exogenous plant miRNAs in consumers [32–35]. For example, some groups mined public high-throughput sequencing data sets of animal fluids and

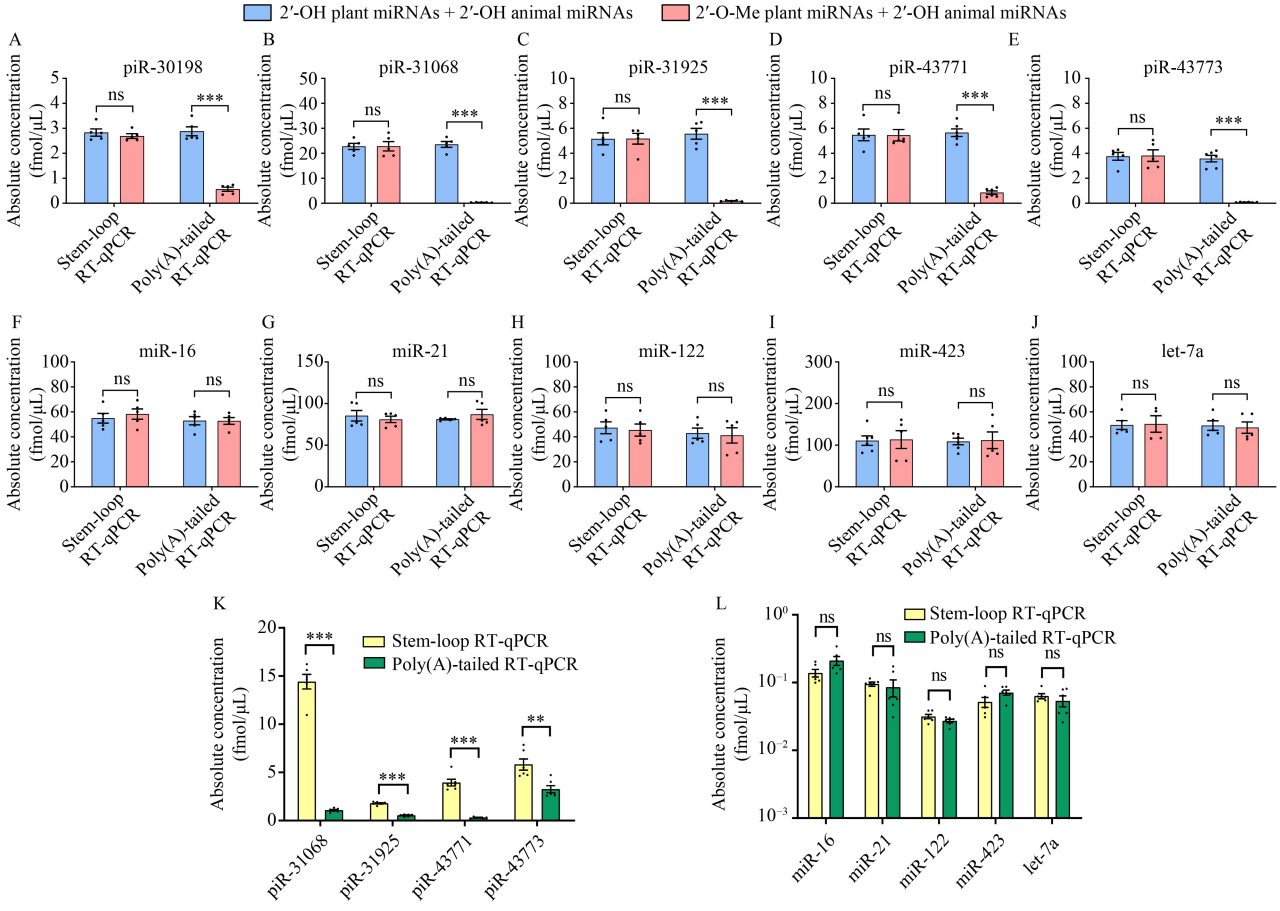

Fig. 4 Comparison of the differences between stem-loop and poly(A)-tailed RT-qPCR in quantifying synthetic 2′-O-methyl piRNAs and piRNAs in seminal plasma. (A–E) The absolute levels of 5 synthetic 2′-O-methyl and 2′-OH piRNAs (e.g., piR-30198, piR-31068, piR-31925, piR-43771, and piR-42773) detected by stem-loop and poly(A)-tailed RT-qPCR. (F–J) The absolute levels of 5 synthetic 2′-OH animal miRNAs (e.g., miR-16, miR-21, miR-122, miR-423, and let-7a) detected by stem-loop and poly(A)-tailed RT-qPCR. (K) The absolute levels of piRNAs (e.g., piR-31068, piR-31925, piR-43771, and piR-42773) determined by stem-loop and poly(A)-tailed RT-qPCR in seminal plasma. (L) The absolute levels of animal miRNAs (e.g., miR-16, miR-21, miR-122, miR-423, and let-7a) determined by stem-loop and poly(A)-tailed RT-qPCR in seminal plasma. Data are represented as the mean ± SEM ($n = 6$). $^{**}P < 0.01$, $^{***}P < 0.001$.

tissues and identified quite small amounts of plant miRNAs in these samples. Therefore, they concluded that plant miRNAs are derived from contaminants during library preparation and sequencing [48]. However, these studies ignored the critical fact that the conventional protocols and solutions in sequencing procedures are biased against plant miRNAs compared with nonmodified animal miRNAs. In other words, if a sample contains a mixture of 2′-O-methyl plant miRNAs and 2′-OH animal miRNAs, ligations will favor the capture of 2′-OH animal miRNAs [22]. Unsurprisingly, the sequencing reads of plant miRNAs are lost in the vast amount of animal miRNAs during the sequencing of mixed plant and animal libraries. Indeed, we obtained few reads of plant miRNAs using a routine sequencing protocol, but an increase in the relative abundances of plant miRNAs was observed in periodate-treated samples. Furthermore, we obtained higher sequencing efficiency with 90 min of oxidation than 40 min, which indicates that the oxidation time and intensity are crucial in 3′-terminal 2′-O-methylated small RNA sequencing. In conclusion, oxidative deep sequencing may be an ideal strategy to detect 3′-terminal 2′-O-methyl small RNAs when they were mixed with unmethylated RNAs, such as in detecting dietary plant miRNAs in animal tissues or piRNAs in circulation.

Currently, the major reported function of piRNAs is to provide an elaborate system that protects germline cells against harmful expression of transposable elements and stabilizes the formation of male germ cells [49,50]. In addition, piRNAs are also shown to be promising prognostic markers for various types of cancers [51]. Efficient and accurate quantification of piRNAs is critical for elucidating their molecular functions. However, piRNAs are notoriously difficult to detect by sequencing or RT-qPCR because of challenges, such as low abundance, assembly in clusters, and 3′-terminal 2′-O-methyl modification. For example, our previous studies surveyed piRNA profiling by deep sequencing technology and detected quite low piRNA levels (~0.5% of total small

RNA sequencing reads) in seminal plasma compared with the significantly enriched miRNAs (~5% of total small RNA sequencing reads). In contrast, the stem-loop RT-qPCR assay determined the concentration of piRNAs at approximately 1–10 000 pmol/L in seminal plasma, which is considerably more abundant than that of miRNAs at about 10–2000 fmol/L [23]. This inconsistency indicates that piRNAs are not accurately assessed ordinarily. To measure the true abundance of piRNAs efficiently, we used oxidized deep sequencing again to overcome the inhibitory effect of 3′-terminal 2′-O-methylation on adaptor ligation. As a result, an increase in the relative abundance of piRNAs in periodate-treated RNAs derived from seminal plasma was detected. Furthermore, we showed that piRNAs can be directly quantified by the stem-loop RT-qPCR assay rather than the poly(A)-tailed RT-qPCR assay. Overall, the combination of oxidative deep sequencing with stem-loop RT-qPCR may provide a nonbiased technique to measure piRNAs with 3′-terminal 2′-O-methylation accurately.

In conclusion, this study established a standard procedure for quantifying the levels of 3′-terminal 2′-O-methylated small RNAs, including plant miRNAs and piRNAs. With the ubiquitous presence of 3′-terminal 2′-O-methyl modifications across a wide variety of species, the accurate detection of 3′-terminal 2′-O-methylated small RNAs is critical to understand their basic biological principles and has profound clinical implications.

Acknowledgements

This work was supported by the Fundamental Research Funds for the Central Universities (No. 020814380146), National Basic Research Program of China (973 Program) (No. 2014CB542300), National Natural Science Foundation of China (Nos. 32022015, 32001077, 31871295, 21877060, 81250044, 81602697, and 81772727), and Research Unit of Extracellular Non-Coding RNA, Chinese Academy of Medical Sciences (No. 2021RU015).

Compliance with ethics guidelines

Yan Kong, Huanhuan Hu, Yangyang Shan, Zhen Zhou, Ke Zen, Yulu Sun, Rong Yang, Zheng Fu, and Xi Chen declare that they have no conflict of interest. The study protocol was approved by the Institutional Review Board of Nanjing University (Nanjing, China) (Approval No. IACUC-2006008). All procedures followed were in accordance with the ethical standards of the responsible committee on human experimentation (institutional and national) and with the *Helsinki Declaration* of 1975, as revised in 2000 (5). Informed consent was obtained from all patients who provided semen samples.

Electronic Supplementary Material Supplementary material is available in the online version of this article at https://doi.org/10.1007/s11684-021-0909-7 and is accessible for authorized users.

References

1. Limbach PA, Crain PF, McCloskey JA. Summary: the modified nucleosides of RNA. Nucleic Acids Res 1994; 22(12): 2183–2196
2. Motorin Y, Helm M. RNA nucleotide methylation. Wiley Interdiscip Rev RNA 2011; 2(5): 611–631
3. Machnicka MA, Milanowska K, Osman Oglou O, Purta E, Kurkowska M, Olchowik A, Januszewski W, Kalinowski S, Dunin-Horkawicz S, Rother KM, Helm M, Bujnicki JM, Grosjean H. MODOMICS: a database of RNA modification pathways—2013 update. Nucleic Acids Res 2013; 41(Database issue D1): D262−D267
4. Kirino Y, Mourelatos Z. 2′-O-methyl modification in mouse piRNAs and its methylase. Nucleic Acids Symp Ser (Oxf) 2007(51): 417–418
5. Shen Y, Zheng KX, Duan D, Jiang L, Li J. Label-free microRNA profiling not biased by 3' end 2'-O-methylation. Anal Chem 2012; 84(15): 6361–6365
6. Xie Z, Khanna K, Ruan S. Expression of microRNAs and its regulation in plants. Semin Cell Dev Biol 2010; 21(8): 790–797
7. Bartel DP. MicroRNAs: genomics, biogenesis, mechanism, and function. Cell 2004; 116(2): 281–297
8. Yu B, Yang Z, Li J, Minakhina S, Yang M, Padgett RW, Steward R, Chen X. Methylation as a crucial step in plant microRNA biogenesis. Science 2005; 307(5711): 932–935
9. Vagin VV, Sigova A, Li C, Seitz H, Gvozdev V, Zamore PD. A distinct small RNA pathway silences selfish genetic elements in the germline. Science 2006; 313(5785): 320–324
10. Kwon C, Tak H, Rho M, Chang HR, Kim YH, Kim KT, Balch C, Lee EK, Nam S. Detection of PIWI and piRNAs in the mitochondria of mammalian cancer cells. Biochem Biophys Res Commun 2014; 446(1): 218–223
11. Siomi MC, Sato K, Pezic D, Aravin AA. PIWI-interacting small RNAs: the vanguard of genome defence. Nat Rev Mol Cell Biol 2011; 12(4): 246–258
12. Horwich MD, Li C, Matranga C, Vagin V, Farley G, Wang P, Zamore PD. The *Drosophila* RNA methyltransferase, DmHen1, modifies germline piRNAs and single-stranded siRNAs in RISC. Curr Biol 2007; 17(14): 1265–1272
13. Kamminga LM, Luteijn MJ, den Broeder MJ, Redl S, Kaaij LJT, Roovers EF, Ladurner P, Berezikov E, Ketting RF. Hen1 is required for oocyte development and piRNA stability in zebrafish. EMBO J 2010; 29(21): 3688–3700
14. Kirino Y, Mourelatos Z. The mouse homolog of HEN1 is a potential methylase for Piwi-interacting RNAs. RNA 2007; 13(9): 1397–1401
15. Saito K, Sakaguchi Y, Suzuki T, Suzuki T, Siomi H, Siomi MC. Pimet, the *Drosophila* homolog of HEN1, mediates 2′-O-methylation of Piwi-interacting RNAs at their 3′ ends. Genes Dev 2007; 21(13): 1603–1608
16. Chen X. Small RNAs and their roles in plant development. Annu Rev Cell Dev Biol 2009; 25(1): 21–44
17. Ahlquist P. RNA-dependent RNA polymerases, viruses, and RNA silencing. Science 2002; 296(5571): 1270–1273
18. Kirino Y, Mourelatos Z. Mouse Piwi-interacting RNAs are 2′-O-methylated at their 3′ termini. Nat Struct Mol Biol 2007; 14(4): 347–348
19. Kurth HM, Mochizuki K. 2′-O-methylation stabilizes Piwi-associated small RNAs and ensures DNA elimination in *Tetrahymena*. RNA 2009; 15(4): 675–685

20. Ameres SL, Horwich MD, Hung JH, Xu J, Ghildiyal M, Weng Z, Zamore PD. Target RNA-directed trimming and tailing of small silencing RNAs. Science 2010; 328(5985): 1534–1539
21. Aschenbrenner J, Marx A. Direct and site-specific quantification of RNA 2′-O-methylation by PCR with an engineered DNA polymerase. Nucleic Acids Res 2016; 44(8): 3495–3502
22. Munafó DB, Robb GB. Optimization of enzymatic reaction conditions for generating representative pools of cDNA from small RNA. RNA 2010; 16(12): 2537–2552
23. Hong Y, Wang C, Fu Z, Liang H, Zhang S, Lu M, Sun W, Ye C, Zhang CY, Zen K, Shi L, Zhang C, Chen X. Systematic characterization of seminal plasma piRNAs as molecular biomarkers for male infertility. Sci Rep 2016; 6(1): 24229
24. Zhang L, Hou D, Chen X, Li D, Zhu L, Zhang Y, Li J, Bian Z, Liang X, Cai X, Yin Y, Wang C, Zhang T, Zhu D, Zhang D, Xu J, Chen Q, Ba Y, Liu J, Wang Q, Chen J, Wang J, Wang M, Zhang Q, Zhang J, Zen K, Zhang CY. Exogenous plant MIR168a specifically targets mammalian LDLRAP1: evidence of cross-kingdom regulation by microRNA. Cell Res 2012; 22(1): 107–126
25. Zhu K, Liu M, Fu Z, Zhou Z, Kong Y, Liang H, Lin Z, Luo J, Zheng H, Wan P, Zhang J, Zen K, Chen J, Hu F, Zhang CY, Ren J, Chen X. Plant microRNAs in larval food regulate honeybee caste development. PLoS Genet 2017; 13(8): e1006946
26. Zhou Z, Li X, Liu J, Dong L, Chen Q, Liu J, Kong H, Zhang Q, Qi X, Hou D, Zhang L, Zhang G, Liu Y, Zhang Y, Li J, Wang J, Chen X, Wang H, Zhang J, Chen H, Zen K, Zhang CY. Honeysuckle-encoded atypical microRNA2911 directly targets influenza A viruses. Cell Res 2015; 25(1): 39–49
27. Chin AR, Fong MY, Somlo G, Wu J, Swiderski P, Wu X, Wang SE. Cross-kingdom inhibition of breast cancer growth by plant miR159. Cell Res 2016; 26(2): 217–228
28. Liang G, Zhu Y, Sun B, Shao Y, Jing A, Wang J, Xiao Z. Assessing the survival of exogenous plant microRNA in mice. Food Sci Nutr 2014; 2(4): 380–388
29. Mlotshwa S, Pruss GJ, MacArthur JL, Endres MW, Davis C, Hofseth LJ, Peña MM, Vance V. A novel chemopreventive strategy based on therapeutic microRNAs produced in plants. Cell Res 2015; 25(4): 521–524
30. Yang J, Farmer LM, Agyekum A A A, Elbaz-Younes I, Hirschi KD. Detection of an abundant plant-based small RNA in healthy consumers. PLoS One 2015; 10(9): e0137516
31. Yang J, Farmer LM, Agyekum A A A, Hirschi KD. Detection of dietary plant-based small RNAs in animals. Cell Res 2015; 25(4): 517–520
32. Dickinson B, Zhang Y, Petrick JS, Heck G, Ivashuta S, Marshall WS. Lack of detectable oral bioavailability of plant microRNAs after feeding in mice. Nat Biotechnol 2013; 31(11): 965–967
33. Masood M, Everett CP, Chan SY, Snow JW. Negligible uptake and transfer of diet-derived pollen microRNAs in adult honey bees. RNA Biol 2016; 13(1): 109–118
34. Tosar JP, Rovira C, Naya H, Cayota A. Mining of public sequencing databases supports a non-dietary origin for putative foreign miRNAs: underestimated effects of contamination in NGS. RNA 2014; 20(6): 754–757
35. Micó V, Martín R, Lasunción MA, Ordovás JM, Daimiel L. Unsuccessful detection of plant microrNAs in beer, extra virgin olive oil and human plasma after an acute ingestion of extra virgin olive oil. Plant Foods Hum Nutr 2016; 71(1): 102–108
36. Ji L, Chen X. Regulation of small RNA stability: methylation and beyond. Cell Res 2012; 22(4): 624–636
37. Ohara T, Sakaguchi Y, Suzuki T, Ueda H, Miyauchi K, Suzuki T. The 3′ termini of mouse Piwi-interacting RNAs are 2′-O-methylated. Nat Struct Mol Biol 2007; 14(4): 349–350
38. Chen X, Ba Y, Ma L, Cai X, Yin Y, Wang K, Guo J, Zhang Y, Chen J, Guo X, Li Q, Li X, Wang W, Zhang Y, Wang J, Jiang X, Xiang Y, Xu C, Zheng P, Zhang J, Li R, Zhang H, Shang X, Gong T, Ning G, Wang J, Zen K, Zhang J, Zhang CY. Characterization of microRNAs in serum: a novel class of biomarkers for diagnosis of cancer and other diseases. Cell Res 2008; 18(10): 997–1006
39. Haldipur B, Arankalle V. Circulating miR-122 levels in self-recovering hepatitis E patients. ExRNA 2019; 1: 2
40. Wang N, Qu S, Sun W, Zeng Z, Liang H, Zhang CY, Chen X, Zen K. Direct quantification of 3′ terminal 2′-*O*-methylation of small RNAs by RT-qPCR. RNA 2018; 24(11): 1520–1529
41. Zhao C, Sun X, Li L. Biogenesis and function of extracellular miRNAs. ExRNA 2019; 1: 38
42. Jiang X, Hou D, Wei Z, Zheng S, Zhang Y, Li J. Extracellular and intracellular microRNAs in pancreatic cancer: from early diagnosis to reducing chemoresistance. ExRNA 2019; 1: 17
43. Perera BPU, Tsai ZT, Colwell ML, Jones TR, Goodrich JM, Wang K, Sartor MA, Faulk C, Dolinoy DC. Somatic expression of piRNA and associated machinery in the mouse identifies short, tissue-specific piRNA. Epigenetics 2019; 14(5): 504–521
44. Tang W, Tu S, Lee HC, Weng Z, Mello CC. The ribonuclease PARN-1 trims piRNA 3′ ends to promote transcriptome surveillance in *C. elegans*. Cell 2016; 164(5): 974–984
45. Sellitto A, Geles K, D'Agostino Y, Conte M, Alexandrova E, Rocco D, Nassa G, Giurato G, Tarallo R, Weisz A, Rizzo F. Molecular and functional characterization of the somatic PIWIL1/piRNA pathway in colorectal cancer cells. Cells 2019; 8(11): 1390
46. Tang F, Hayashi K, Kaneda M, Lao K, Surani MA. A sensitive multiplex assay for piRNA expression. Biochem Biophys Res Commun 2008; 369(4): 1190–1194
47. Honda S, Loher P, Morichika K, Shigematsu M, Kawamura T, Kirino Y, Rigoutsos I, Kirino Y. Increasing cell density globally enhances the biogenesis of Piwi-interacting RNAs in *Bombyx mori* germ cells. Sci Rep 2017; 7(1): 4110
48. Kang W, Bang-Berthelsen CH, Holm A, Houben AJS, Müller AH, Thymann T, Pociot F, Estivill X, Friedländer MR. Survey of 800+ data sets from human tissue and body fluid reveals xenomiRs are likely artifacts. RNA 2017; 23(4): 433–445
49. Tóth KF, Pezic D, Stuwe E, Webster A. The piRNA pathway guards the germline genome against transposable elements. Adv Exp Med Biol 2016; 886: 51–77
50. Zhao K, Cheng S, Miao N, Xu P, Lu X, Zhang Y, Wang M, Ouyang X, Yuan X, Liu W, Lu X, Zhou P, Gu J, Zhang Y, Qiu D, Jin Z, Su C, Peng C, Wang JH, Dong MQ, Wan Y, Ma J, Cheng H, Huang Y, Yu Y. A Pandas complex adapted for piRNA-guided transcriptional silencing and heterochromatin formation. Nat Cell Biol 2019; 21(10): 1261–1272
51. Sun T, Han X. The disease-related biological functions of PIWI-interacting RNAs (piRNAs) and underlying molecular mechanisms. ExRNA 2019; 1: 21